



Interleukin-21 Induces Short-Lived Effector CD8⁺ T Cells but Does Not Inhibit Their Exhaustion after *Mycobacterium bovis* BCG Infection in Mice

Naoto Noguchi,^a Risa Nakamura,^{a,b} Shinya Hatano,^a Hisakata Yamada,^a Xun Sun,^c Naoya Ohara,^d Yasunobu Yoshikai^a

^aDivision of Host Defense, Medical Institute of Bioregulation, Kyushu University, Fukuoka, Japan

^bDepartment of Parasitology, Institute of Tropical Medicine, Nagasaki University, Nagasaki, Japan

^cDepartment of Immunology, China Medical University, Shenyang, China

^dDepartment of Oral Microbiology, Graduate School of Medicine, Dentistry and Pharmaceutical Sciences, Okayama University, Okayama, Japan

ABSTRACT Interleukin 21 (IL-21) is a pleiotropic common cytokine receptor γ chain cytokine that promotes the effector functions of NK cells and CD8⁺ T cells and inhibits CD8⁺ T cell exhaustion during chronic infection. We found that the absolute number of short-lived effector CD8⁺ T cells (SLECs) (KLRG1^{high} CD127^{low}) decreased significantly in IL-21 receptor-deficient (IL-21R^{-/-}) mice during *Mycobacterium bovis* bacillus Calmette-Guérin (BCG) infection. Early effector CD8⁺ T cells (EECs) (KLRG1^{low} CD127^{low}) were normally generated in IL-21R^{-/-} mice after infection. Exhausted CD8⁺ T cells (PD-1^{high} KLRG1^{low}) were also normally generated in IL-21R^{-/-} mice after infection. Mixed bone marrow (BM) chimera and transfer experiments showed that IL-21R on CD8⁺ T cells was essential for the proliferation of EECs, allowing them to differentiate into SLECs after BCG infection. On the other hand, the number of SLECs increased significantly after infection with recombinant BCG (rBCG) that secreted an antigen 85B (Ag85B)-IL-21 fusion protein (rBCG-Ag85B-IL-21), but the number of exhausted CD8⁺ T cells did not change after rBCG-Ag85B-IL-21 infection. These results suggest that IL-21 signaling drives the differentiation of SLECs from EECs but does not inhibit the exhaustion of CD8⁺ T cells following BCG infection in mice.

KEYWORDS IL-21R, CD8 T cells, SLECs, EECs, PD-1

A member of the interleukin 2 (IL-2) family cytokines, IL-21, which utilizes the IL-21 receptor (IL-21R) and a common cytokine receptor γ chain (CD132) for signal transduction, is secreted mainly by activated CD4⁺ T cells and natural killer (NK) T cells (1–8). IL-21R is widely expressed on various cell types within the immune system, including CD8⁺ cytotoxic T cells and CD4⁺ T follicular helper (Tfh) cells (9–18). The widespread lymphoid distribution of IL-21R leads to the pleiotropic action of IL-21 in innate and adaptive immune responses (4–9). Several lines of evidence show the effects of IL-21 on antigen (Ag)-specific CD8⁺ T cell proliferation and effector function. IL-21R-deficient (IL-21R^{-/-}) mice showed an impaired Ag-specific CD8⁺ T cell response after immunization with vaccinia virus expressing gp160 (19) or after infection with *Mycobacterium tuberculosis* (20) or *Encephalitozoon cuniculi* (21). However, the primary Ag-specific CD8⁺ T cell response in acute infection with lymphocytic choriomeningitis virus (LCMV) or *Listeria monocytogenes* appears to proceed independently of IL-21, since fairly similar initial responses are elicited in the presence and absence of IL-21 (22–24).

The pools of effector CD8⁺ T cells at an early stage after infection are divided into two main subsets, short-lived effector cells (SLECs) and memory precursor effector cells

Received 27 February 2018 Returned for modification 29 March 2018 Accepted 18 May 2018

Accepted manuscript posted online 29 May 2018

Citation Noguchi N, Nakamura R, Hatano S, Yamada H, Sun X, Ohara N, Yoshikai Y. 2018. Interleukin-21 induces short-lived effector CD8⁺ T cells but does not inhibit their exhaustion after *Mycobacterium bovis* BCG infection in mice. *Infect Immun* 86:e00147-18. <https://doi.org/10.1128/IAI.00147-18>.

Editor Sabine Ehrh, Weill Cornell Medical College

Copyright © 2018 American Society for Microbiology. All Rights Reserved.

Address correspondence to Yasunobu Yoshikai, yoshikai@bioreg.kyushu-u.ac.jp.

N.N. and R.N. contributed equally to this article.

(MPECs), based on the expression of KLRG1 and CD127. SLECs are in fact KLRG1^{high} CD127^{low} cells that form terminally differentiated effector cells. MPECs are KLRG1^{low} CD127^{high} cells that differentiate into long-lived memory cells (25–27). In addition to these two subsets, early effector cells (EECs) were recently found to have a KLRG1^{low} CD127^{low} phenotype, with the ability to form both SLECs and MPECs (28, 29). However, the inflammatory stimuli that alter their fate remain unknown.

Sustained antigenic stimulation associated with persistent infection may often cause CD8⁺ T cell exhaustion, which is characterized by functional unresponsiveness, the expression of multiple inhibitory receptors, such as CD43 (1B11 isoform), and maintained expression of the inhibitory receptors programmed death 1 (PD-1), lymphocyte-activated gene 3 (LAG-3), T-cell immunoglobulin and mucin domain-containing protein 3 (TIM-3), and cytotoxic T-lymphocyte-associated protein 4 (CTLA-4) (30–32). It has been reported recently that IL-21 inhibited CD8⁺ T cell exhaustion, controlling chronic infection by LCMV (22) or *M. tuberculosis* (20). However, whether IL-21 directly inhibits the development of CD8⁺ T cell exhaustion remains unknown.

In this study, we used IL-21R^{-/-} mice and IL-21-expressing recombinant *Mycobacterium bovis* bacillus Calmette-Guérin (rBCG–Ag85B–IL-21), with rBCG expressing ovalbumin (OVA), to examine the roles of IL-21 in the Ag-specific CD8⁺ T cell response in the lung following BCG infection. We found that IL-21 signaling played a critical role in converting EECs to SLECs but was not involved in inhibiting the generation of exhausted CD8⁺ T cells after BCG infection in mice.

RESULTS

Kinetics of bacterial load and cytokine production in IL-21R^{-/-} mice after BCG infection. We first examined bacterial numbers and cytokine production in the lungs. The number of bacteria was slightly higher in IL-21R^{-/-} mice than in wild-type (WT) mice on day 14 after rBCG-OVA infection but decreased equally in both groups thereafter (Fig. 1A). The level of IL-21 was higher in IL-21R^{-/-} mice than in WT mice during rBCG-OVA infection (Fig. 1B), presumably due to the lack of IL-21 consumption. The level of gamma interferon (IFN- γ) was significantly lower in IL-21R^{-/-} mice than in WT mice on day 28 after rBCG-OVA infection (Fig. 1B). There were no differences in the levels of IL-10 and IL-17A between WT mice and IL-21R^{-/-} mice during infection (Fig. 1B).

CD8⁺ T cell response in IL-21R^{-/-} mice after BCG infection. We next examined CD8⁺ T cell responses in the lungs and spleens after rBCG-OVA infection. OVA_{257–264} H-2K^b tetramer staining revealed that the absolute numbers of OVA-specific CD8⁺ T cells decreased in the lungs and spleens of IL-21R^{-/-} mice on days 14 and 21 after rBCG-OVA infection (Fig. 2A; see also Fig. S1A in the supplemental material). Intracellular staining for IFN- γ upon OVA_{257–264} stimulation showed that the ability of OVA-specific CD8⁺ T cells from rBCG-OVA-infected IL-21R^{-/-} mice to produce IFN- γ was significantly lower than that of WT mice on days 21 and 42 after rBCG-OVA infection (Fig. 2B; also Fig. S1B in the supplemental material).

Ag-specific CD8⁺ T cells can be classified into several categories: C44⁻ CD62L⁺ naïve cells, CD44⁺ CD62L⁻ effector or effector memory cells, and CD44⁺ CD62L⁺ central memory T cells (33, 34). The majority of OVA-specific CD8⁺ T cells were of the CD44⁺ CD62L⁻ phenotype in both groups, and the absolute numbers of OVA-specific CD44⁺ CD62L⁻ CD8⁺ T cells in the lungs and spleens were significantly lower in IL-21R^{-/-} mice than in WT mice on days 14 and 21 after rBCG-OVA infection (Fig. 3A; see also Fig. S2A in the supplemental material). The absolute numbers of OVA-specific CD44⁺ CD62L⁺ CD8⁺ T cells were significantly lower in IL-21R^{-/-} mice on day 21 (Fig. 3A). The pools of effector CD8⁺ T cells at an early stage after infection were further divided into three subsets—EECs, SLECs, and MPECs—based on the expression of KLRG1 and CD127 (27–29, 33, 34). The majority of OVA-specific CD8⁺ T cells had the KLRG1^{high} CD127^{low} phenotype, corresponding to SLECs, in WT mice on days 14 and 21 after rBCG-OVA infection (Fig. 3B; also Fig. S2B in the supplemental material). The numbers of SLECs were significantly lower in the lungs and spleens of IL-21R^{-/-} mice

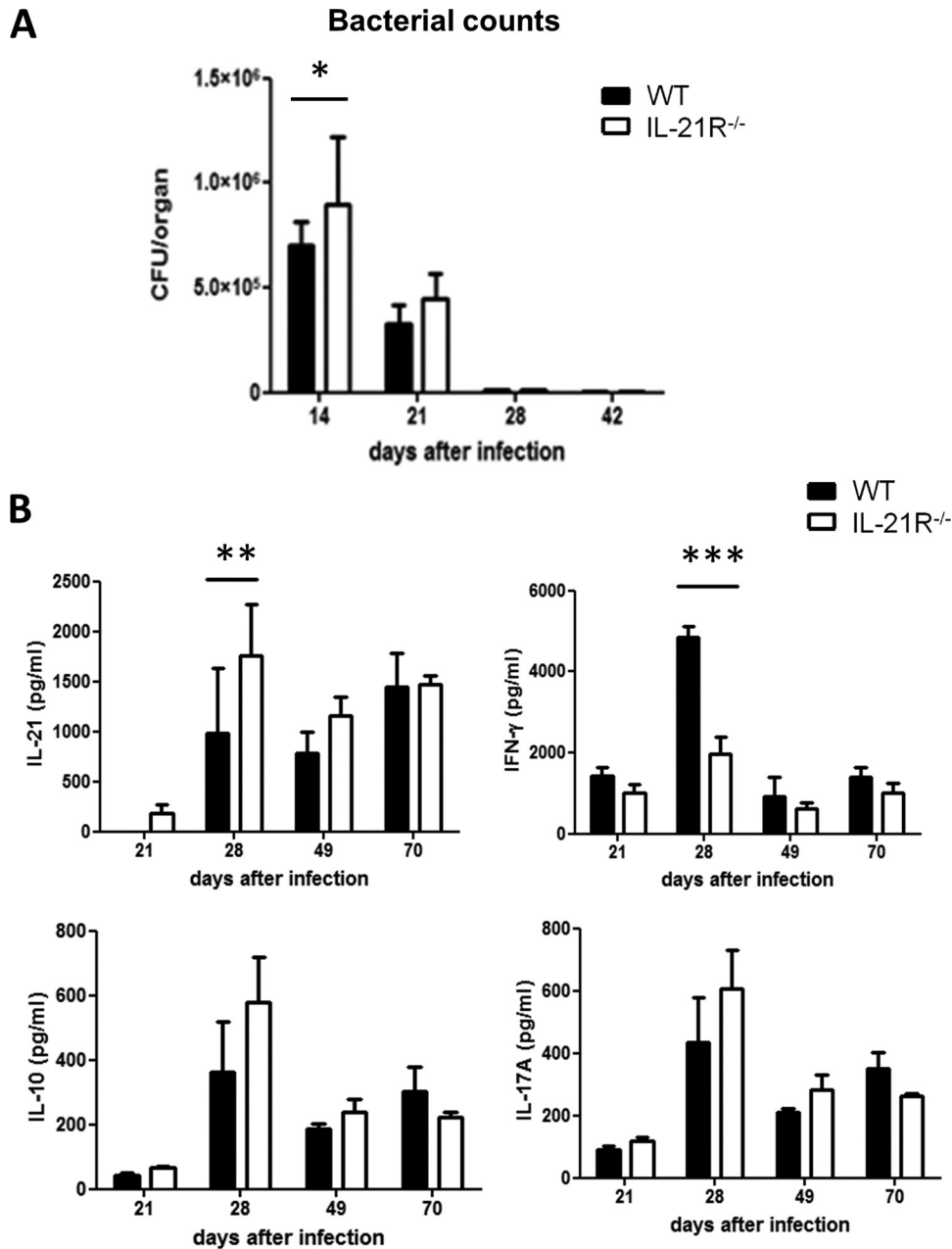


FIG 1 Kinetics of bacterial growth and cytokine production in the lungs of IL-21R^{-/-} mice after BCG infection. IL-21R^{-/-} mice and age-matched wild-type (WT) mice were infected i.t. with 2 × 10⁶ CFU of rBCG-OVA. (A) The numbers of bacteria recovered from the lungs of infected mice were determined on the indicated days. (B) Cytokine production in lung homogenates from mice at the indicated times after rBCG-OVA infection. IL-21, IFN-γ, IL-10, and IL-17A levels in the lung homogenates were measured by ELISA. Data from one experiment representative of three separate experiments are shown and are expressed as means ± standard deviations for five mice from each group. Statistically significant differences between IL-21R^{-/-} mice and WT mice are indicated (*, *P* < 0.05; **, *P* < 0.01; ***, *P* < 0.001).

than in those of WT mice on days 14 and 21 (Fig. 3B). The relative percentage of EECs increased in IL-21R^{-/-} mice (Fig. S2B), but the absolute number was comparable to that in WT mice after infection (Fig. 3B).

Two transcription factors, T-bet and Blimp-1, are highly expressed in SLECs (27, 35, 36), whereas another two, Bcl-6 and eomesodermin (Eomes), are important in MPEC differentiation (37–41). In agreement with the reduced number of SLECs in IL-21R^{-/-} mice, the mean fluorescence intensities (MFI) of T-bet and Blimp-1 expressed by the

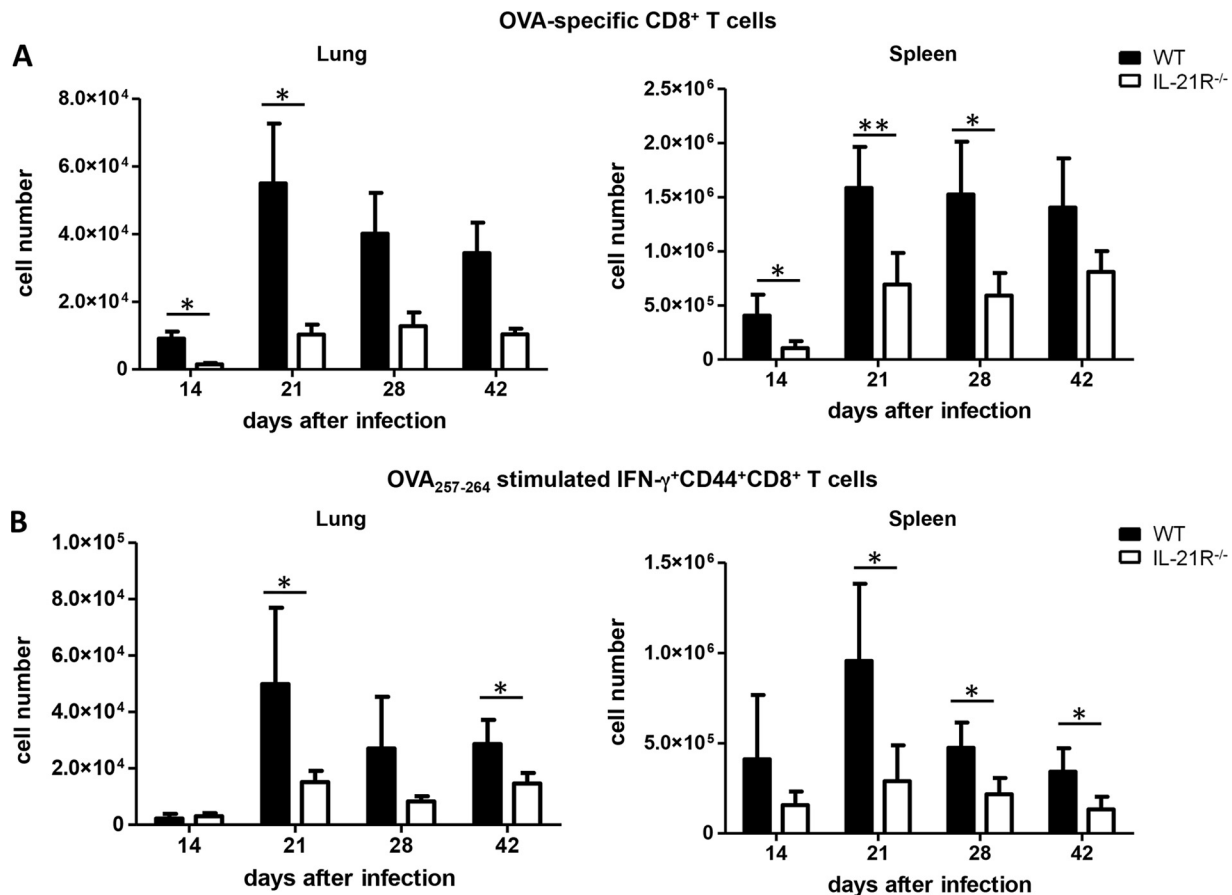


FIG 2 Kinetics of Ag-specific CD8⁺ T cells and IFN-γ⁺ CD8⁺ T cells in IL-21R^{-/-} mice following BCG infection. (A) The absolute number of OVA₂₅₇₋₂₆₄-specific CD8⁺ T cells was calculated by multiplying the total number of lung MNCs or spleen cells by the percentage of each subset. On the indicated days after infection with 2×10^6 CFU of rBCG-OVA, the lung MNCs and spleen cells of each mouse were stained with an anti-CD8 MAb and OVA₂₅₇₋₂₆₄ H-2K^b tetramers. (B) The absolute number of OVA₂₅₇₋₂₆₄-specific IFN-γ⁺ CD8⁺ T cells was calculated by multiplying the total number of lung MNCs or spleen cells by the percentage of IFN-γ⁺ CD44⁺ CD8⁺ T cells. For intracellular expression of IFN-γ by CD44⁺ CD8⁺ T cells, the lung MNCs or spleen cells were cultured with the OVA₂₅₇₋₂₆₄ peptide on the indicated days after rBCG-OVA infection and were surface stained with an anti-CD8 and an anti-CD44 MAb and intracellularly stained with an anti-IFN-γ MAb. Data from one experiment representative of three separate experiments are shown. Each value shown is the mean \pm standard deviation for four mice of each group. Statistically significant differences between IL-21R^{-/-} mice and WT mice are indicated (*, $P < 0.05$; **, $P < 0.01$).

OVA-specific CD8⁺ T cells were significantly reduced in IL-21R^{-/-} mice infected with rBCG-OVA (Fig. 3C; also Fig. S2C in the supplemental material). There were no differences in the MFI of Bcl-6 and Eomes between the two groups of mice (Fig. 3C; also Fig. S2C). Taking these findings together, the differentiation of SLECs from EECs may be inhibited in the absence of IL-21R signaling.

Exhausted CD8⁺ T cells in IL-21R^{-/-} mice after BCG infection. Exhausted T cells show phenotypic features of an exhausted state, including upregulated expression of inhibitory receptors such as PD-1 (30–32). We examined PD-1 expression on OVA-specific CD8⁺ T cells following rBCG-OVA infection. The percentage of OVA-specific PD-1^{high} KLRG1^{low} CD8⁺ T cells, corresponding to exhausted T cells, was higher in the lungs of IL-21R^{-/-} mice than in those of WT mice 21 days after rBCG-OVA infection (Fig. S2D in the supplemental material). However, the absolute numbers of OVA-specific PD-1^{high} KLRG1^{low} CD8⁺ T cells in the lungs of IL-21R^{-/-} mice were not significantly different from those in WT mice after rBCG-OVA infection (Fig. 3D). The higher proportion of exhausted T cells among OVA-specific CD8⁺ T cells in IL-21R^{-/-} mice may reflect a change in the total number of OVA-specific effector CD8⁺ T cells in IL-21R^{-/-} mice.

Direct effect of IL-21R signaling on the CD8⁺ T cell response after BCG infection. IL-21R is widely expressed on various cell types within the immune system (9–17).

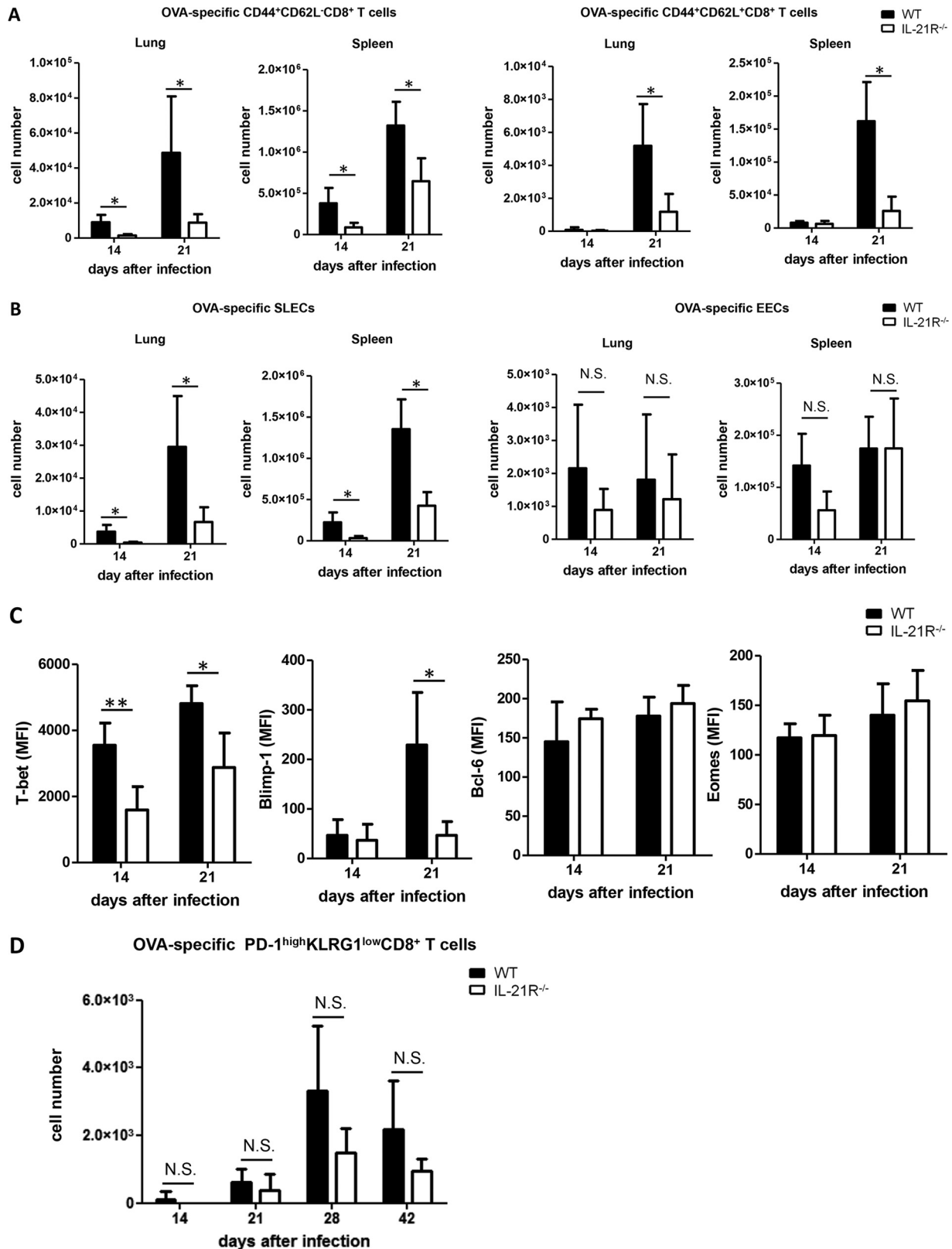


FIG 3 Kinetics of numbers of Ag-specific effector CD8⁺ T cells in IL-21R^{-/-} mice following BCG infection. (A and B) The absolute number of OVA-specific CD44⁺ CD62L⁻ CD8⁺ T cells, CD44⁺ CD62L⁺ CD8⁺ T cells, short-lived effector cells (SLECs), or early effector cells (EECs) was calculated by multiplying the total number of lung MNCs or spleen cells by the percentage of each subset. On the indicated days after infection with 2×10^6 CFU of rBCG-OVA, the lung MNCs and spleen cells were stained either with anti-CD8, anti-CD44, and anti-CD62L MABs and OVA₂₅₇₋₂₆₄ H-2K^b tetramers or with anti-CD8, anti-KLRG1, and anti-CD127 MABs and OVA₂₅₇₋₂₆₄ H-2K^b tetramers. (C) The mean fluorescence (Continued on next page)

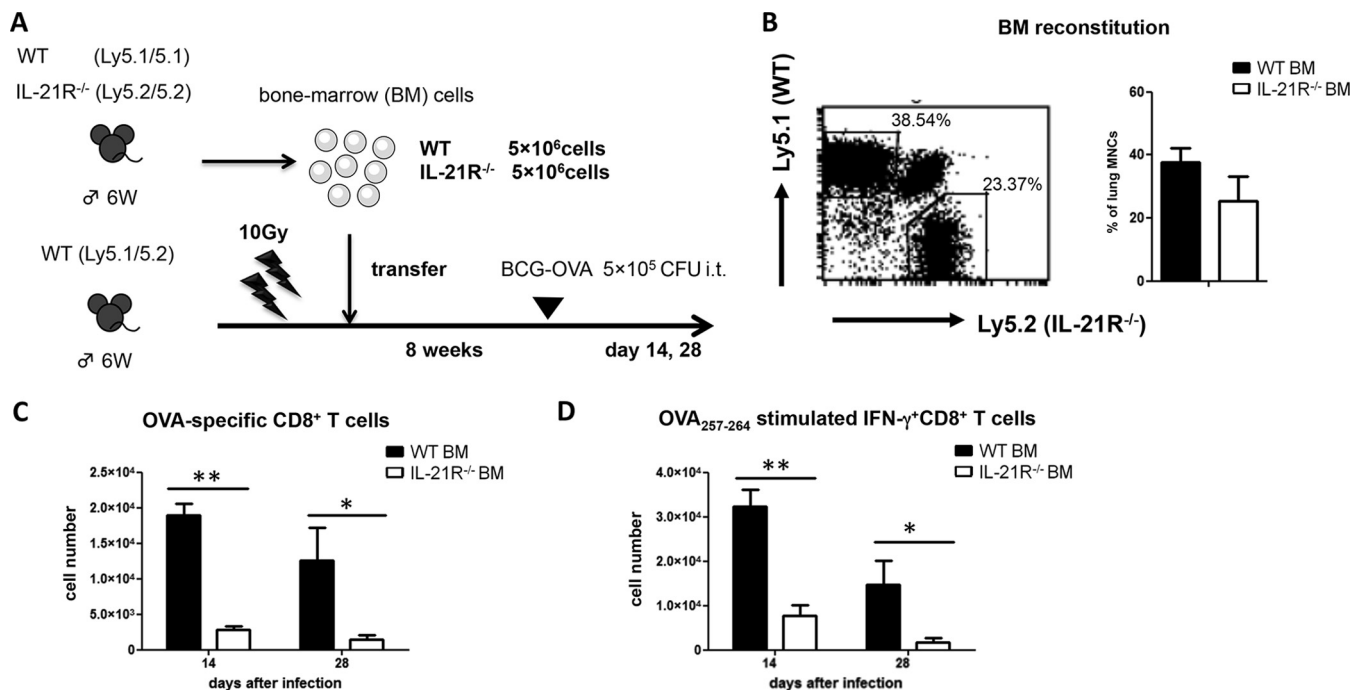


FIG 4 IL-21R signaling for differentiation of Ag-specific CD8⁺ T cells in mixed bone marrow (BM) chimeric mice following BCG infection. (A) Recipient WT (Ly5.1/5.2) mice were lethally irradiated (10 Gy), and BM was reconstituted by a mixture of WT (Ly5.1/5.1) and IL-21R^{-/-} (Ly5.2/5.2) BM cells. Eight weeks after BM transfer, 5 × 10⁵ CFU rBCG-OVA was i.t. inoculated, and the lung cells were harvested on days 14 and 28 after infection. (B) Eight weeks after BM transfer, the lung cells were stained with an anti-Ly5.1 and an anti-Ly5.2 MAb. (C) The absolute number of OVA_{257–264}-specific CD8⁺ T cells expressing Ly5.1/5.1 or Ly5.2/5.2 was calculated by multiplying the total number of lung MNCs by the percentage of each subset. The lung MNCs were stained with anti-CD8, anti-Ly5.1, and anti-Ly5.2 MAbs and OVA_{257–264} H-2K^b tetramers. (D) The absolute number of OVA_{257–264}-specific IFN-γ⁺ CD8⁺ T cells was calculated by multiplying the total number of lung MNCs by the percentage of IFN-γ⁺ CD8⁺ T cells. For intracellular expression of IFN-γ by CD8⁺ T cells, lung MNCs were cultured with the OVA_{257–264} peptide on the indicated days after rBCG-OVA infection, surface stained with anti-CD8, anti-Ly5.1, and anti-Ly5.2 MAbs, and intracellularly stained with an anti-IFN-γ MAb. Data from one experiment representative of two separate experiments are shown. Each value shown is the mean ± standard deviation for three mice. Statistically significant differences between IL-21R^{-/-} and WT T cells are indicated (*, P < 0.05; **, P < 0.01).

To determine whether IL-21R was acting directly on Ag-specific CD8⁺ T cells or indirectly, through a third party, we first performed a mixed bone marrow (BM) chimera experiment using Ly5.1- or Ly5.2-congenic C57BL/6 (B6) mice. Recipient WT mice (Ly5.1/5.2) were lethally irradiated and injected with a mixture of BM cells from WT (Ly5.1/5.1) and IL-21R^{-/-} (Ly5.2/5.2) mice (Fig. 4A). Cells derived from IL-21R^{-/-} BM and WT BM were equally distributed in host mice 2 months after BM transplantation (Fig. 4B). On days 14 and 28 after rBCG-OVA infection, the numbers of OVA-specific CD8⁺ T cells from IL-21R^{-/-} mice were significantly lower than those from WT mice in BM chimeric mice (Fig. 4C). Moreover, the ability of OVA-specific CD8⁺ T cells from IL-21R^{-/-} mice to produce IFN-γ was significantly lower than that of cells from WT mice (Fig. 4D). These results suggest that IL-21R on BM-derived cells is critical for the differentiation or expansion of Ag-specific CD8⁺ T cells after BCG infection.

To further confirm the requirement for IL-21R expression by Ag-specific CD8⁺ T cells, we carried out transfer experiments using OT-I cells, which express an OVA-specific T cell receptor (TCR). WT or IL-21R^{-/-} naïve OT-I cells were transferred to WT mice, which were then challenged with rBCG-OVA, and the number of OT-I cells in the lungs was

FIG 3 Legend (Continued)

intensities (MFI) of T-bet, Blimp-1, Bcl-6, and Eomes in OVA_{257–264}-specific CD8⁺ T cells in the lung were calculated on days 14 and 21 after rBCG-OVA infection. For intracellular expression of T-bet, Blimp-1, Bcl-6, and Eomes by OVA_{257–264}-specific CD8⁺ T cells, lung MNCs were surface stained with an anti-CD8 MAb and OVA_{257–264} H-2K^b tetramers and were intracellularly stained with each MAb. (D) The absolute number of OVA_{257–264}-specific exhausted CD8⁺ T cells was calculated by multiplying the total number of lung MNCs by the percentage of the PD-1^{high} KLRG1^{low} subset. On the indicated days after infection with 2 × 10⁶ CFU of rBCG-OVA, lung MNCs were stained with anti-CD8, anti-KLRG1, and anti-PD-1 MAbs and OVA_{257–264} H-2K^b tetramers. Data from one experiment representative of three separate experiments are shown. Each value shown is the mean ± standard deviation for four mice of each group. Statistically significant differences between IL-21R^{-/-} mice and WT mice are indicated (*, P < 0.05; **, P < 0.01). N.S., not significant.

examined on day 14 (Fig. 5A). IL-21R^{+/+} and IL-21R^{-/-} OT-I cells were equally distributed in host mice after adoptive transfer, while the number of IL-21R^{-/-} OT-I cells in the lungs and mediastinal lymph nodes (MLNs) was significantly lower than that of WT OT-I cells on day 14 after rBCG-OVA infection (Fig. 5B and C). The percentages and absolute numbers of SLECs were significantly reduced in IL-21R^{-/-} OT-I cells after infection (Fig. 5D and E). The percentage of EECs showed a relative increase in IL-21R^{-/-} OT-I cells (Fig. 5D), but there was no significant difference in the absolute number of EECs between IL-21R^{+/+} and IL-21R^{-/-} OT-I cells after infection (Fig. 5E). Thus, IL-21R is important for the generation of effector CD8⁺ T cells in the lymphoid organs after BCG infection.

To examine the *in vivo* division of OT-I cells, OT-I cells were labeled with 1 μ M 5-(and-6)-carboxyfluorescein diacetate succinimidyl ester (CFSE) and were injected intravenously (i.v.) into WT mice, which were subsequently injected with 2×10^6 CFU rBCG-OVA. Transfer of CFSE-labeled OT-I cells showed that cell division on day 14 after rBCG-OVA infection was impaired in IL-21R^{-/-} OT-I cells relative to that in WT OT-I cells (Fig. 5F). These results indicate that IL-21R signaling in CD8⁺ T cells is indispensable for their proliferation and for the differentiation of OVA-specific SLECs from EECs in the lungs after BCG infection.

CD8⁺ T cell response after rBCG–Ag85B–IL-21 infection. To elucidate the effects of IL-21 on CD8⁺ T cell responses to BCG infection under conditions of IL-21 overexpression, we used rBCG–IL-21–Ag85B, secreting the IL-21–Ag85B fusion protein, which can be detected by an enzyme-linked immunosorbent assay (ELISA) with an anti-IL-21 monoclonal antibody (MAb) (42). The level of TB10.4- or Mtb32a-specific CD8⁺ T cells was examined after intratracheal (i.t.) inoculation with 5×10^4 CFU rBCG–Ag85B–IL-21 or rBCG–Ag85B. There was no difference in bacterial counts in the lungs between rBCG–Ag85B–IL-21- and rBCG–Ag85B-infected mice (Fig. 6A). The numbers of TB10.4- or Mtb32a-specific CD8⁺ T cells, as assessed by tetramer staining, were significantly higher on day 21 after rBCG–Ag85B–IL-21 infection (Fig. 6B; see also Fig. S3A in the supplemental material). Similarly, the numbers of IFN- γ ⁺ CD44⁺ CD8⁺ T cells upon stimulation with the TB10.4 or Mtb32a peptide were significantly higher on day 21 after rBCG–Ag85B–IL-21 infection (Fig. 6C; also Fig. S3B in the supplemental material). Most of the TB10.4- or Mtb32a-specific CD8⁺ T cells showed the KLRG1^{high} CD127^{low} phenotype, corresponding to SLECs (Fig. S3C). The numbers of TB10.4- or Mtb32a-specific SLECs were significantly higher on day 21 after rBCG–Ag85B–IL-21 infection (Fig. 6D). Although the relative number of PD-1^{high} KLRG1^{low} exhausted CD8⁺ T cells decreased after rBCG–Ag85B–IL-21 infection (Fig. S3D), the absolute numbers of rBCG–Ag85B–IL-21- and rBCG–Ag85B-infected mice were not different (Fig. 6E). These results suggest that overproduction of IL-21 increases the number of SLECs but does not affect the generation of exhausted CD8⁺ T cells.

DISCUSSION

In this study, we show two novel findings pertaining to the role of IL-21 in the CD8⁺ T cell response during BCG infection: (i) IL-21 signaling plays a critical role in the proliferation and differentiation of SLECs from EECs; (ii) IL-21 by itself may have very little, if any, effect on the generation of exhausted CD8⁺ T cells (see Fig. S4 in the supplemental material).

Effector CD8⁺ T cells at an early stage after acute infection are divided into two subsets: KLRG1^{high} CD127^{low} SLECs, which differentiate into terminally differentiated effector cells, and KLRG1^{low} CD127^{high} MPECs, which differentiate into long-lived memory cells (27–29, 33, 34). In the present study, the number of SLECs decreased significantly in IL-21R^{-/-} mice on days 14 and 21 after rBCG-OVA infection and vice versa, i.e., there was a significant increase in the number of SLECs after rBCG–Ag85B–IL-21 infection. These results suggest that IL-21 had a positive impact on the quality of the effector CD8⁺ T cell response during chronic infection by BCG. IL-21R is widely expressed on various cells (9–18) and leads to the pleiotropic action of IL-21 in innate and adaptive immune responses. In the present study, the double approach of using

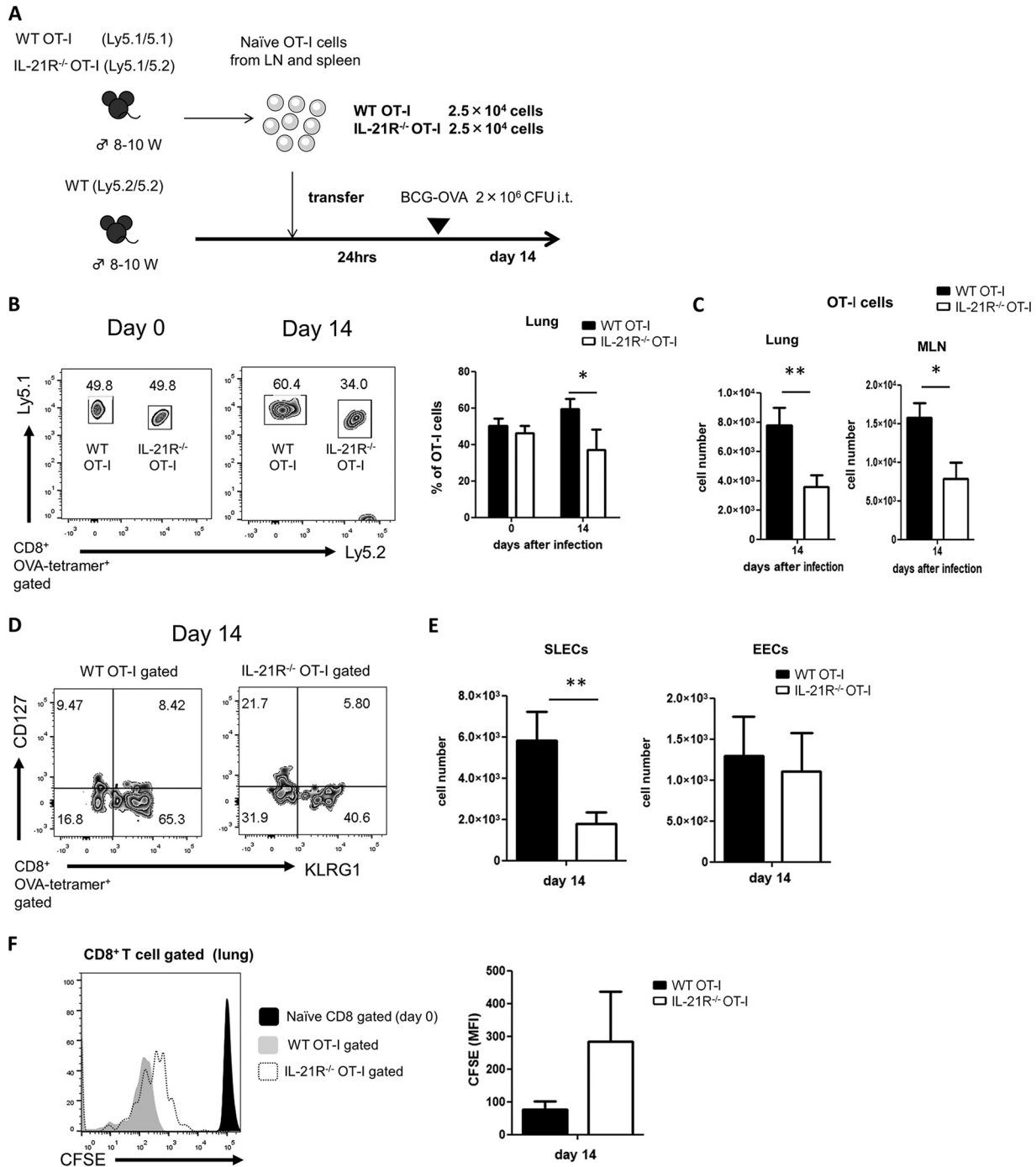


FIG 5 IL-21R signaling for differentiation of Ag-specific CD8⁺ T cells in adoptive transfer experiments following BCG infection. (A) Naïve CD8⁺ T cells purified from WT (Ly5.1/5.1) and IL-21R^{-/-} (Ly5.1/5.2) OT-I mice were transferred i.v. into WT mice (Ly5.2/5.2), which were inoculated i.t. with 2 × 10⁶ CFU rBCG-OVA on the next day. Two weeks after infection, lungs were harvested. (B) Percentages of OT-I cells in the lung after rBCG-OVA infection. (C) The absolute number of OT-I cells expressing Ly5.1/5.1 or Ly5.1/5.2 was calculated by multiplying the total number of lung MNCs or mediastinal lymph node (MLN) cells by the percentage of each subset. On day 14 after infection, the lung MNCs and MLNs were stained with anti-CD8, anti-Ly5.1, and anti-Ly5.2 MAbs and OVA₂₅₇₋₂₆₄ H-2K^b tetramers. (D) Numbers in the dot plot show the percentage of each region in a gated population. A representative fluorescence-activated cell sorter profile is shown. On day 14 after infection, lung MNCs were stained with anti-CD8, anti-Ly5.1, anti-Ly5.2, anti-CD127, and anti-KLRG1 MAbs and OVA₂₅₇₋₂₆₄ H-2K^b tetramers. (E) The absolute number of SLECs or EECs was calculated by multiplying the total number of lung MNCs by the percentage of each subset. (F) Histogram overlays of CFSE on CD8⁺ T cells. Shown are levels for naïve CD8⁺ T cells before transfer (filled histogram), WT OT-I CD8⁺ T cells after infection (shaded histogram), and IL-21R^{-/-} OT-I CD8⁺ T cells after infection (open histogram). The MFI of CFSE in WT or IL-21R^{-/-} OT-I CD8⁺ T cells was calculated on day 14 after rBCG-OVA infection. To examine the division of OT-I cells *in vivo*, the cells were first labeled with 1 μM CFSE and then injected intravenously into sex-matched WT mice, which were subsequently injected with 2 × 10⁶ CFU rBCG-OVA. On day 14 after infection, lung MNCs were stained with anti-CD8, anti-Ly5.1, and anti-Ly5.2 MAbs. Data from one experiment representative of two separate experiments are shown. Each value shown is the mean ± standard deviation for four mice. Statistically significant differences between IL-21R^{-/-} OT-I CD8⁺ T cells and WT OT-I CD8⁺ T cells are indicated (*, P < 0.05; **, P < 0.01).

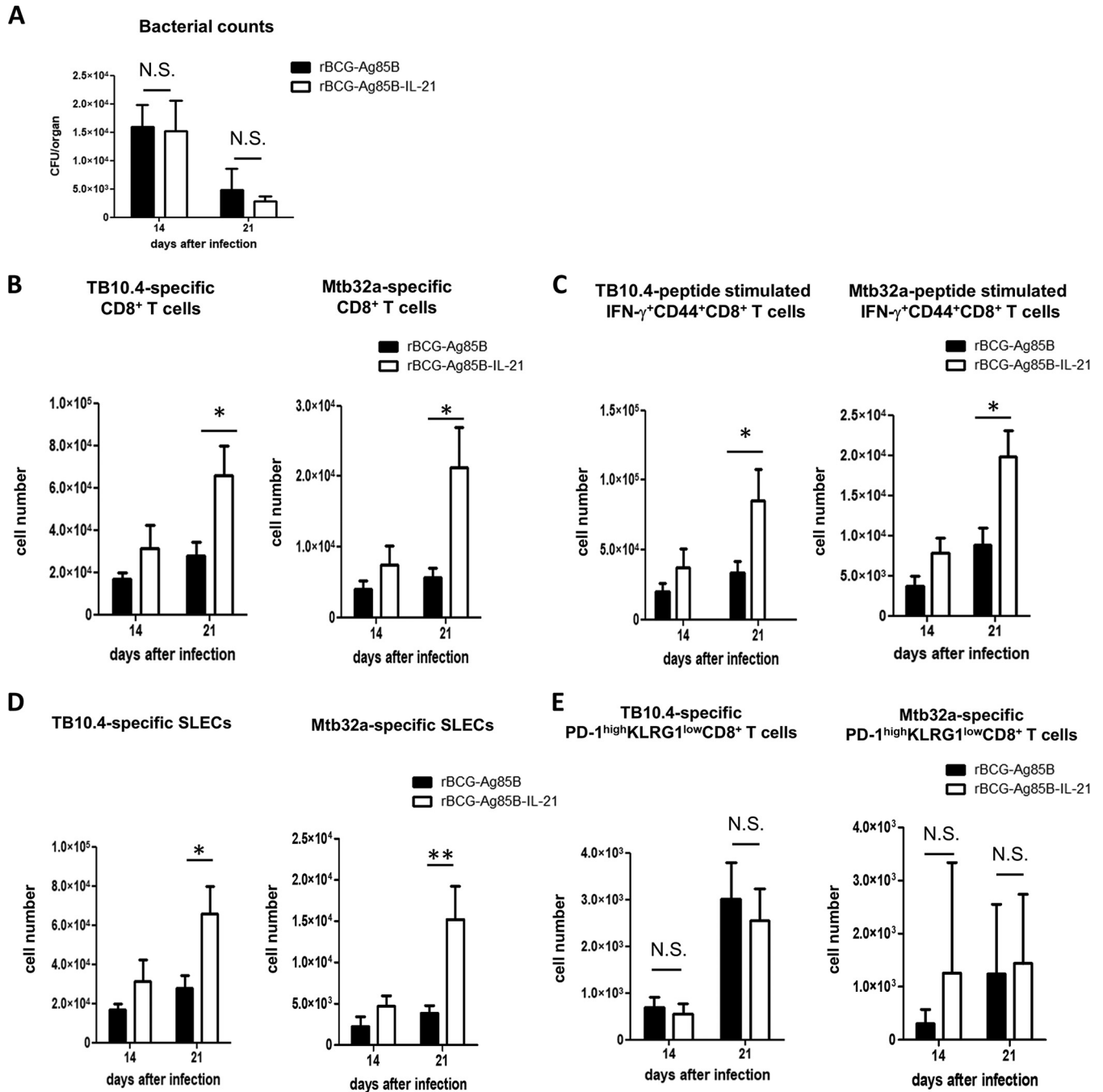


FIG 6 Kinetics of Ag-specific CD8⁺ T cells following rBCG-Ag85B-IL-21 inoculation. The lung MNCs were harvested on the indicated days, at an early stage after rBCG-Ag85B-IL-21 or rBCG-Ag85B inoculation. (A) The numbers of bacteria recovered from the lungs of infected mice on the indicated days were determined. (B) The absolute numbers of TB10.4- or Mtb32a-specific CD8⁺ T cells were determined by staining with an anti-CD8 MAb and TB10.4 or an Mtb32a MHC class I tetramer. (C to E) The absolute numbers of TB10.4- or Mtb32a-specific IFN- γ ⁺ CD44⁺ CD8⁺ T cells were calculated by multiplying the total number of lung MNCs by the percentage of IFN- γ ⁺ CD44⁺ CD8⁺ T cells stimulated with the TB10.4 or Mtb32a peptide. The lung MNCs were stained with an anti-CD8, anti-KLRG1, anti-CD127, or anti-PD-1 MAb and TB10.4 or Mtb32a MHC class I tetramers. Data from one experiment representative of three separate experiments are shown. Each value shown is the mean \pm standard deviation for four mice of each group. Asterisks indicate statistically significant differences between rBCG-Ag85B-IL-21-infected mice and rBCG-Ag85B-infected mice (*, $P < 0.05$; **, $P < 0.01$). N.S., not significant.

mixed BM chimeras and adoptive transfer indicates that direct signaling from IL-21R on CD8⁺ T cells contributes to the proliferation and differentiation of the effector CD8⁺ T cell response against BCG infection. These results were consistent with a previous report on *M. tuberculosis* infection (20), although the loss of IL-21R has almost no effect on bacterial elimination after rBCG-OVA infection. This may be explained by the

difference in virulence between rBCG-OVA and *M. tuberculosis*. Effector cells other than CD8⁺ T cells may compensate for the absence of effector CD8⁺ T cells in IL-21R^{-/-} mice following avirulent rBCG-OVA infection.

Obar and colleagues recently showed that KLRG1^{low} CD127^{low} EECs appear at a very early stage, such as day 3 after acute infection with recombinant *Listeria*-OVA or recombinant vesicular stomatitis virus (rVSV)-OVA (28, 29). They also showed that EECs have the ability to form both SLECs and MPECs but that this depends on pathogen-induced inflammatory environmental conditions (28). We showed in our study that EECs appeared at a relatively early stage (day 14) in chronic bacterial infection with rBCG-OVA. Notably, in contrast to SLECs, the absolute number of EECs in IL-21R^{-/-} mice after infection did not differ from that in WT mice. During the response of CD8⁺ T cells to infection, SLECs express high levels of T-bet and Blimp-1, whereas MPECs express high levels of Bcl-6 and Eomes (27, 35–41). The balance of expression of T-bet, Blimp-1, Bcl-6, and Eomes is important for the efficient development of CD8⁺ T cells. In accord with the decreased number of SLECs in IL-21R^{-/-} mice, the expression of T-bet and Blimp-1 in Ag-specific CD8⁺ T cells was lower in IL-21R^{-/-} mice than in WT mice at an early phase of infection. These results suggest that IL-21 is a critical factor for the proliferation and differentiation of EECs into SLECs at a relatively early stage (day 14) of chronic infection with BCG.

The roles of IL-21 in Ag-specific CD8⁺ T cell proliferation and effector function are controversial. The Ag-specific CD8⁺ T cell response in acute infection with LCMV or *L. monocytogenes* appears to proceed independently of IL-21, since the initial CD8⁺ T cell responses are elicited in IL-21^{-/-} mice at the same level as in WT mice (22–24). Conversely, the response of CD8⁺ T cells is impaired in IL-21^{-/-} or IL-21R^{-/-} mice during chronic infection with strains of LCMV or *M. tuberculosis* (20, 22). In agreement with those reports, we showed that the effector CD8⁺ T cell response deteriorated in the absence of IL-21R signaling. Taking these findings together, it is possible that the effects of IL-21 on the Ag-specific effector CD8⁺ T cell response may differ between acute and chronic infection, irrespective of the pathogen (viral or bacterial). An apparent difference in the adaptive immune response between acute and chronic infection is the interval required for its development. *L. monocytogenes* proliferated rapidly *in vivo*, resulting in rapid Ag presentation with a formidable CD8⁺ T cell response, which peaked on day 7, but subsequently, T cells underwent rapid apoptosis. In contrast, BCG grows slowly, resulting in delayed Ag presentation and a weaker magnitude of the CD8⁺ T cell response, which peaks around the second week of infection and then declines slowly (43, 44). IL-21 induces KLRG1 expression but inhibits CD94-NKG2A expression on NK cells *in vitro*, resulting in functional maturation of NK cells (10). IL-21R activates Jak1 and Jak2, causing the phosphorylation, dimerization, and nuclear translocation of Stat3 and, to a lesser extent, Stat1, Stat5a, and Stat5b (3–8, 45). The balance of activation of these STAT proteins may influence the expression of IL-21-regulated genes in CD8⁺ T cells after infection. Further experiments are required to clarify how IL-21 induces KLRG1 during effector maturation of CD8⁺ T cells.

It has been reported recently that CD8⁺ T cells become exhausted in chronic viral infection under conditions of persistent Ag stimulation, conditions that arise during chronic infection with HIV, LCMV, or *M. tuberculosis* and in cancer (30–32). Effector activities, including the ability to produce IFN- γ , are lost by the exhausted CD8⁺ T cells, and the absolute number of these cells declines. The exhausted T cells also express phenotypic features of the exhausted state, including PD-1, CTLA-4, LAG-3, and Tim-3 (29–32). Chronic LCMV infection of IL-21^{-/-} or IL-21R^{-/-} mice results in severe CD8⁺ T cell exhaustion, proving the importance of IL-21 in sustaining CD8⁺ T cell responses during chronic viral infection (22). Thus, the availability of IL-21 critically influences the functional quality and sustainability of CD8⁺ T cell responses, especially under conditions of persistent Ag stimulation during chronic infections (20, 29). CD8⁺ T cell exhaustion can develop if IL-21 is unavailable, indicating that the level of IL-21 influences the capacity to mount effective responses. However, we did not detect an increase in the absolute number of PD-1^{high} CD8⁺ T cells in IL-21R^{-/-} mice, although

the relative percentage of PD-1^{high} CD8⁺ T cells increased after BCG infection. We also did not detect a decrease in the absolute number of PD-1^{high} CD8⁺ T cells, although the relative number of PD-1^{high} CD8⁺ T cells decreased after rBCG–Ag85B–IL-21 infection. The downregulation of inhibitory receptors by IL-21 signaling may merely reflect IL-21-induced expansion of effector CD8⁺ T cells in BCG infection. It was therefore predicted that IL-21 would not have a positive impact on the quality of the exhausted CD8⁺ T cell response after chronic infection with BCG. There are several mechanisms for processing Ag for major histocompatibility complex (MHC) class I presentation, such as proteasomal processing in classical cytosol processing by infected antigen-presenting cells (APC) and cross-processing by bystander APC (46). Therefore, it is also possible that differences in Ag-processing mechanisms for MHC class I presentation among various chronic infections may affect IL-21 function in the quality of the exhausted CD8⁺ T cell response. The generalizability of our finding and its possible implications await analysis of other chronic infections.

In conclusion, IL-21 plays an important role in the CD8⁺ T cell response in BCG infection. Ensuing important steps will be the use of our improved understanding of the roles of IL-21 to devise approaches to vaccination for tuberculosis.

MATERIALS AND METHODS

Mice. C57BL/6 wild-type (WT) mice were purchased from Japan KBT Inc. (Tosu, Japan). IL-21R^{-/-} mice were generated as described previously (9). OT-I mice expressing an ovalbumin (OVA)_{257–264}/K^b-specific TCR and B6 Ly5.1-congenic mice were obtained from the Jackson Laboratory (Bar Harbor, ME). All mice were maintained under specific-pathogen-free conditions and were provided food and water *ad libitum*. All mice used were 6 to 12 weeks old. This study was approved by the Committee of Ethics on Animal Experiments of the Faculty of Medicine, Kyushu University. Experiments were carried out according to local guidelines for animal experimentation.

Microorganisms. OVA-expressing recombinant BCG (rBCG-OVA) has been described previously (43). To construct rBCG–Ag85B–IL-21 or rBCG–Ag85B, pNN2–mIL-21–Ag85B or pNN2–Ag85B was introduced into BCG (strain Tokyo 172) by electroporation as reported previously (42, 44, 47).

Bacterial infection. The culture method for rBCG-OVA, rBCG–Ag85B–IL-21, or rBCG–Ag85B has been described previously (42, 48). Mice were inoculated intratracheally (i.t.) with viable *M. bovis* BCG (Tokyo strain) or rBCG-OVA in 50 μ l of phosphate-buffered saline (PBS) on day 0 at a sublethal dose of 5×10^4 or 2×10^6 CFU. On various days after infection, mouse lungs were removed and separately homogenized. Samples were spread on Middlebrook 7H10 medium enriched with 10% oleic acid-albumin-dextrose-catalase (OADC), and colonies were counted after incubation for 3 weeks at 37°C.

Flow cytometric analysis. Lung mononuclear cells (MNCs), spleen cells, and MLNs were prepared as described previously (49, 50). All cells were stained with various combinations of MAbs. I-A/I-E-V500 (M5.144.15.2), allophycocyanin- and Cy.7-conjugated CD8 α (RM53-6.7), CD44-V450 (IM7), phycoerythrin (PE)- and Cy.7-conjugated CD127 (A7R34), Alexa Fluor 488-conjugated Bcl-6 (K112-91), Alexa Fluor 647-conjugated Blimp-1 (5E7), and PE- and Cy.7-conjugated streptavidin antibodies were purchased from BD Biosciences (San Jose, CA). Peridinin chlorophyll protein (PerCP)- and Cy5.5-conjugated CD44 (clone IM7), PerCP- and Cy5.5-conjugated CD45.1 (A20), PE- and Cy.7-conjugated CD45.2 and fluorescein isothiocyanate (FITC)-conjugated CD45.2C (clone 104), PerCP- and Cy5.5-conjugated CD62L (MEL-14), PE-conjugated IL-21R (4A9), allophycocyanin-conjugated KLRG1 and PerCP- and Cy5.5-conjugated KLRG1 (2F1/KLRG1), biotin-conjugated PD-1 (RMP1-30), and allophycocyanin-conjugated T-bet (4B10) antibodies were purchased from BioLegend (San Diego, CA). Biotin-conjugated CD45.2 (A20) and Alexa Fluor 488-conjugated Eomes (Dan11mag) antibodies were purchased from eBioscience (San Diego, CA). PE-conjugated OVA_{257–264} H-2K^b, TB10.4 H-2K^b, and Mtb32a H-2D^b tetramers were purchased from MBL (Nagoya, Japan). Dead cells were excluded from the analysis using a Zombie Aqua fixable viability kit (BioLegend). Intracellular staining with T-bet, Blimp-1, Bcl-6, and Eomes was performed with the Foxp3 staining kit (eBioscience). The stained cells were analyzed in a FACSVerser flow cytometer (BD Biosciences). The data were analyzed using FlowJo software, v10.0.7 (TreeStar).

Intracellular cytokine staining. Lung MNCs or spleen cells were incubated without any stimulation or with each peptide (5 μ g/ml OVA_{257–264}, 10 μ M TB10.4, or 10 μ M Mtb32a) or 1 μ g/ml phorbol 12-myristate 13-acetate (PMA) plus 50 μ g/ml ionomycin (ION) for 6 h, with 10 μ g/ml brefeldin A (Sigma-Aldrich) added in the last 3 h, at a concentration of 1×10^5 in RPMI 1640 medium containing 10% fetal calf serum (FCS). After culture, cells were preincubated with the 2.4G2 antibody and were stained with various combinations of MAbs. After surface staining, intracellular staining was performed using the Cytotfix/Cytoperm kit (BD Biosciences).

ELISAs. Supernatants of lung homogenates from mice were obtained by centrifugation at $440 \times g$ for 3 min at 4°C. Cytokine secretion in the supernatants was measured with a DuoSet ELISA development system (R&D Systems, Minneapolis, MN) according to the manufacturer's protocol.

Generation of mixed bone marrow chimera. BM cells were prepared from WT (Ly5.1/5.1) and IL-21R^{-/-} (Ly5.2/5.2) mice by flushing the femurs and tibiae and resuspending them in PBS for injection. A mixture of 2×10^6 cells from WT (Ly5.1/5.1) and IL-21R^{-/-} (Ly5.2/5.2) mice was injected intravenously (i.v.) into lethally (10-Gy) irradiated WT recipient mice (Ly5.1/5.2).

Adoptive transfer. Adoptive transfer cells were obtained from spleen and lymph node (LN) cells in IL21R^{+/+} OT-I mice (Ly5.1/5.1) or IL21R^{-/-} OT-I mice (Ly5.1/5.2). OT-I naïve CD8⁺ T cells that had been negatively purified using magnetic beads (EasySep naïve CD8⁺ T cell isolation kit; Stemcell Technologies, Vancouver, Canada) were mixed (2.5×10^4 cells from each group) and adoptively transferred i.v. into naïve B6 mice (Ly5.2/5.2), which were infected with 2×10^6 CFU rBCG-OVA 24 h later. Transferred OT-I cells were identified by staining with various combinations of MAbs and OVA_{257–264} H-2K^b tetramers. In some experiments, OT-I cells were labeled with 1 μ M 5-(and-6)-carboxyfluorescein diacetate succinimidyl ester (CFSE; Invitrogen, Grand Island, NY) in PBS for 15 min at 37°C. After the reaction was stopped by the addition of an equal volume of FCS, the cells were washed with RPMI 1640 medium including 10% FCS.

Statistics. Statistical significance was evaluated by Student's *t* test using Prism software (GraphPad, San Diego, CA). *P* values of <0.05 represent a significant difference.

SUPPLEMENTAL MATERIAL

Supplemental material for this article may be found at <https://doi.org/10.1128/IAI.00147-18>.

SUPPLEMENTAL FILE 1, PDF file, 0.6 MB.

ACKNOWLEDGMENTS

This work was supported by a Grant-in-Aid for Scientific Research on Innovative Areas (JSPS KAKENHI grant JP 16H06496 to Y.Y.).

We declare no conflicts of interest associated with this article.

Y.Y. designed the project, supervised experiments, and wrote the manuscript. N.N. and R.N. performed experiments, analyzed data, and wrote the manuscript. N.N. and R.N. contributed equally to this work and are co-first authors. All other authors contributed to data collection and interpretation and critically reviewed the manuscript. N.O. provided rBCG–Ag85B and rBCG–Ag85B–IL-21.

REFERENCES

- Parrish-Novak J, Dillon SR, Nelson A, Hammond A, Sprecher C, Gross JA, Johnston J, Madden K, Xu W, West J, Schrader S, Burkhead S, Heipel M, Brandt C, Kuijper JL, Kramer J, Conklin D, Presnell SR, Berry J, Shiota F, Bort S, Hambly K, Mudri S, Clegg C, Moore M, Grant FJ, Lofton-Day C, Gilbert T, Rayond F, Ching A, Yao L, Smith D, Webster P, Whitmore T, Maurer M, Kaushansky K, Holly RD, Foster D. 2000. Interleukin 21 and its receptor are involved in NK cell expansion and regulation of lymphocyte function. *Nature* 408:57–63. <https://doi.org/10.1038/35040504>.
- Ozaki K, Kikly K, Michalovich D, Young PR, Leonard WJ. 2000. Cloning of a type I cytokine receptor most related to the IL-2 receptor beta chain. *Proc Natl Acad Sci U S A* 97:11439–11444. <https://doi.org/10.1073/pnas.200360997>.
- Asao H, Okuyama C, Kumaki S, Ishii N, Tsuchiya S, Foster D, Sugamura K. 2001. The common gamma-chain is an indispensable subunit of the IL-21 receptor complex. *J Immunol* 167:1–5. <https://doi.org/10.4049/jimmunol.167.1.1>.
- Mehta DS, Wurster AL, Grusby MJ. 2004. Biology of IL-21 and the IL-21 receptor. *Immunol Rev* 202:84–95. <https://doi.org/10.1111/j.0105-2896.2004.00201.x>.
- Spolski R, Leonard WJ. 2008. Interleukin-21: basic biology and implications for cancer and autoimmunity. *Annu Rev Immunol* 26:57–79. <https://doi.org/10.1146/annurev.immunol.26.021607.090316>.
- Spolski R, Leonard WJ. 2010. IL-21 and T follicular helper cells. *Int Immunol* 22:7–12. <https://doi.org/10.1093/intimm/dxp112>.
- Yi JS, Cox MA, Zajac AJ. 2010. Interleukin-21: a multifunctional regulator of immunity to infections. *Microbes Infect* 12:1111–1119. <https://doi.org/10.1016/j.micinf.2010.08.008>.
- Tian Y, Zajac AJ. 2016. IL-21 and T cell differentiation: consider the context. *Trends Immunol* 37:557–568. <https://doi.org/10.1016/j.it.2016.06.001>.
- Ozaki K, Spolski R, Feng CG, Qi CF, Cheng J, Sher A, Morse HC, III, Liu C, Schwartzberg PL, Leonard WJ. 2002. A critical role for IL-21 in regulating immunoglobulin production. *Science* 298:1630–1634. <https://doi.org/10.1126/science.1077002>.
- Kasaian MT, Whitters MJ, Carter LL, Lowe LD, Jussif JM, Deng B, Johnson KA, Witek JS, Senices M, Konz RF, Wurster AL, Donaldson DD, Collins M, Young DA, Grusby MJ. 2002. IL-21 limits NK cell responses and promotes antigen-specific T cell activation: a mediator of the transition from innate to adaptive immunity. *Immunity* 16:559–569. [https://doi.org/10.1016/S1074-7613\(02\)00295-9](https://doi.org/10.1016/S1074-7613(02)00295-9).
- Brady J, Hayakawa Y, Smyth MJ, Nutt SL. 2004. IL-21 induces the functional maturation of murine NK cells. *J Immunol* 172:2048–2058. <https://doi.org/10.4049/jimmunol.172.4.2048>.
- Strengell M, Matikainen S, Sirén J, Lehtonen A, Foster D, Julkunen I, Sareneva T. 2003. IL-21 in synergy with IL-15 or IL-18 enhances IFN- γ production in human NK and T cells. *J Immunol* 170:5464–5469. <https://doi.org/10.4049/jimmunol.170.11.5464>.
- Monteleone G, Caruso R, Fina D, Peluso I, Gioia V, Stolfi C, Fantini MC, Caprioli F, Tersigni R, Alessandrini L, MacDonald TT, Pallone F. 2006. Control of matrix metalloproteinase production in human intestinal fibroblasts by interleukin 21. *Gut* 55:1774–1780. <https://doi.org/10.1136/gut.2006.093187>.
- Caruso R, Fina D, Peluso I, Fantini MC, Tosti C, Del Vecchio Blanco G, Paoluzi OA, Caprioli F, Andrei F, Stolfi C, Romano M, Ricci V, MacDonald TT, Pallone F, Monteleone G. 2007. IL-21 is highly produced in *Helicobacter pylori*-infected gastric mucosa and promotes gelatinases synthesis. *J Immunol* 178:5957–5965. <https://doi.org/10.4049/jimmunol.178.9.5957>.
- King C, Tangye SG, Mackay CR. 2008. T follicular helper (TFH) cells in normal and dysregulated immune responses. *Annu Rev Immunol* 26:741–766. <https://doi.org/10.1146/annurev.immunol.26.021607.090344>.
- Nurieva R, Yang XO, Martinez G, Zhang Y, Panopoulos AD, Ma L, Schluns K, Tian Q, Watowich SS, Jetten AM, Dong C. 2007. Essential autocrine regulation by IL-21 in the generation of inflammatory T cells. *Nature* 448:480–483. <https://doi.org/10.1038/nature05969>.
- Jin H, Carrio R, Yu A, Malek TR. 2004. Distinct activation signals determine whether IL-21 induces B cell costimulation, growth arrest, or Bim-dependent apoptosis. *J Immunol* 173:657–665. <https://doi.org/10.4049/jimmunol.173.1.657>.
- Brandt K, Bulfone-Paus S, Foster DC, Rückert R. 2003. Interleukin-21 inhibits dendritic cell activation and maturation. *Blood* 102:4090–4098. <https://doi.org/10.1182/blood-2003-03-0669>.
- Zeng R, Spolski R, Finkelstein SE, Oh S, Kovanen PE, Hinrichs CS, Pise-Masison CA, Radonovich MF, Brady JN, Restifo NP, Berzofsky JA, Leonard WJ. 2005. Synergy of IL-21 and IL-15 in regulating CD8⁺ T cell expansion and function. *J Exp Med* 201:139–148. <https://doi.org/10.1084/jem.20041057>.

20. Booty MG, Barreira-Silva P, Carpenter SM, Nunes-Alves C, Jacques MK, Stowell BL, Jayaraman P, Beamer G, Behar SM. 2016. IL-21 signaling is essential for optimal host resistance against *Mycobacterium tuberculosis* infection. *Sci Rep* 6:36720. <https://doi.org/10.1038/srep36720>.
21. Moretto MM, Khan IA. 2016. IL-21 is important for induction of KLRG1⁺ effector CD8⁺ T cells during acute intracellular infection. *J Immunol* 196:375–384. <https://doi.org/10.4049/jimmunol.1501258>.
22. Fröhlich A, Kisielow J, Schmitz I, Freigang S, Shamshiev AT, Weber J, Marsland BJ, Oxenius A, Kopf M. 2009. IL-21R on T cells is critical for sustained functionality and control of chronic viral infection. *Science* 324:1576–1580. <https://doi.org/10.1126/science.1172815>.
23. Ertelt JM, Johans TM, Rowe JH, Way SS. 2010. Interleukin (IL)-21-independent pathogen-specific CD8⁺ T-cell expansion, and IL-21-dependent suppression of CD4⁺ T-cell IL-17 production. *Immunology* 131:183–191. <https://doi.org/10.1111/j.1365-2567.2010.03287.x>.
24. Tian Y, Cox MA, Kahan SM, Ingram JT, Bakshi RK, Zajac AJ. 2016. A context-dependent role for IL-21 in modulating the differentiation, distribution, and abundance of effector and memory CD8⁺ T cell subsets. *J Immunol* 196:2153–2166. <https://doi.org/10.4049/jimmunol.1401236>.
25. Schluns KS, Kieper WC, Jameson SC, Lefrançois L. 2000. Interleukin-7 mediates the homeostasis of naïve and memory CD8⁺ T cells in vivo. *Nat Immunol* 1:426–432. <https://doi.org/10.1038/80868>.
26. Kaech SM, Tan JT, Wherry EJ, Konieczny BT, Surh CD, Ahmed R. 2003. Selective expression of the interleukin 7 receptor identifies effector CD8⁺ T cells that give rise to long-lived memory cells. *Nat Immunol* 4:1191–1198. <https://doi.org/10.1038/ni1009>.
27. Joshi NS, Cui W, Chandele A, Lee HK, Urso DR, Hagman J, Gapin L, Kaech SM. 2007. Inflammation directs memory precursor and short-lived effector CD8⁺ T cell fates via the graded expression of T-bet transcription factor. *Immunity* 27:281–295. <https://doi.org/10.1016/j.immuni.2007.07.010>.
28. Obar JJ, Jellison ER, Sheridan BS, Blair DA, Pham QM, Zickovich JM, Lefrançois L. 2011. Pathogen-induced inflammatory environment controls effector and memory CD8⁺ T cell differentiation. *J Immunol* 187:4967–4978. <https://doi.org/10.4049/jimmunol.1102335>.
29. Plumlee CR, Obar JJ, Colpitts SL, Jellison ER, Haining WN, Lefrançois L, Khanna KM. 2015. Early effector CD8⁺ T cells display plasticity in populating the short-lived effector and memory-precursor pools following bacterial or viral infection. *Sci Rep* 5:12264. <https://doi.org/10.1038/srep12264>.
30. Yi JS, Cox MA, Zajac AJ. 2010. T-cell exhaustion: characteristics, causes and conversion. *Immunology* 129:474–481. <https://doi.org/10.1111/j.1365-2567.2010.03255.x>.
31. Kim PS, Ahmed R. 2010. Features of responding T cells in cancer and chronic infection. *Curr Opin Immunol* 22:223–230. <https://doi.org/10.1016/j.coi.2010.02.005>.
32. Khan N, Vidyarthi A, Amir M, Mushtaq K, Agrewala JN. 2017. T-cell exhaustion in tuberculosis: pitfalls and prospects. *Crit Rev Microbiol* 43:133–141. <https://doi.org/10.1080/1040841X.2016.1185603>.
33. Ahlers JD, Belyakov IM. 2010. Memories that last forever: strategies for optimizing vaccine T-cell memory. *Blood* 115:1678–1689. <https://doi.org/10.1182/blood-2009-06-227546>.
34. Belz GT, Kallies A. 2010. Effector and memory CD8⁺ T cell differentiation: toward a molecular understanding of fate determination. *Curr Opin Immunol* 22:279–285. <https://doi.org/10.1016/j.coi.2010.03.008>.
35. Kallies A, Xin A, Belz GT, Nutt SL. 2009. Blimp-1 transcription factor is required for the differentiation of effector CD8⁺ T cells and memory responses. *Immunity* 31:283–295. <https://doi.org/10.1016/j.immuni.2009.06.021>.
36. Rutishauser RL, Martins GA, Kalachikov S, Chandele A, Parish IA, Meffre E, Jacob J, Calame K, Kaech SM. 2009. Transcriptional repressor Blimp-1 promotes CD8⁺ T cell terminal differentiation and represses the acquisition of central memory T cell properties. *Immunity* 31:296–308. <https://doi.org/10.1016/j.immuni.2009.05.014>.
37. Intlekofer AM, Takemoto N, Wherry EJ, Longworth SA, Northrup JT, Palanivel VR, Mullen AC, Gasink CR, Kaech SM, Miller JD, Gapin L, Ryan K, Russ AP, Lindsten T, Orange JS, Goldrath AW, Ahmed R, Reiner SL. 2005. Effector and memory CD8⁺ T cell fate coupled by T-bet and eomesodermin. *Nat Immunol* 6:1236–1244. <https://doi.org/10.1038/ni1268>.
38. Intlekofer AM, Takemoto N, Kao C, Banerjee A, Schambach F, Northrup JK, Shen H, Wherry EJ, Reiner SL. 2007. Requirement for T-bet in the aberrant differentiation of unhelped memory CD8⁺ T cells. *J Exp Med* 204:2015–2021. <https://doi.org/10.1084/jem.20070841>.
39. Takemoto N, Intlekofer AM, Northrup JT, Wherry EJ, Reiner SL. 2006. IL-12 inversely regulates T-bet and eomesodermin expression during pathogen-induced CD8⁺ T cell differentiation. *J Immunol* 177:7515–7519. <https://doi.org/10.4049/jimmunol.177.11.7515>.
40. Ichii H, Sakamoto A, Hatano M, Okada S, Toyama H, Taki S, Arima M, Kuroda Y, Tokuhisa T. 2002. Role for Bcl-6 in the generation and maintenance of memory CD8⁺ T cells. *Nat Immunol* 3:558–563. <https://doi.org/10.1038/ni802>.
41. Ichii H, Sakamoto A, Kuroda Y, Tokuhisa T. 2004. Bcl6 acts as an amplifier for the generation and proliferative capacity of central memory CD8⁺ T cells. *J Immunol* 173:883–891. <https://doi.org/10.4049/jimmunol.173.2.883>.
42. Huang Y, Matsumura Y, Hatano S, Noguchi N, Murakami T, Iwakura Y, Sun X, Ohara N, Yoshikai Y. 2016. IL-21 inhibits IL-17A-producing $\gamma\delta$ T-cell response after infection with bacillus Calmette-Guérin via induction of apoptosis. *Innate Immun* 22:588–597. <https://doi.org/10.1177/1753425916664125>.
43. Dudani R, Chapdelaine Y, van Faassen H, Smith DK, Shen H, Krishnan L, Sad S. 2002. Multiple mechanisms compensate to enhance tumor-protective CD8⁺ T cell response in the long-term despite poor CD8⁺ T cell priming initially: comparison between an acute versus a chronic intracellular bacterium expressing a model antigen. *J Immunol* 168:5737–5745. <https://doi.org/10.4049/jimmunol.168.11.5737>.
44. Tang C, Yamada H, Shibata K, Maeda N, Yoshida S, Wajjwalku W, Ohara N, Yamada T, Kinoshita T, Yoshikai Y. 2008. Efficacy of recombinant bacille Calmette-Guérin vaccine secreting interleukin-15/antigen 85B fusion protein in providing protection against *Mycobacterium tuberculosis*. *J Infect Dis* 197:1263–1274. <https://doi.org/10.1086/586902>.
45. Liao W, Lin JX, Leonard WJ. 2011. IL-2 family cytokines: new insights into the complex roles of IL-2 as a broad regulator of T helper cell differentiation. *Curr Opin Immunol* 23:598–604. <https://doi.org/10.1016/j.coi.2011.08.003>.
46. Boom WH. 2007. New TB vaccines: is there a requirement for CD8⁺ T cells? *J Clin Invest* 117:2092–2094. <https://doi.org/10.1172/JCI32933>.
47. Hatano S, Tamura T, Umemura M, Matsuzaki G, Ohara N, Yoshikai Y. 2016. Recombinant *Mycobacterium bovis* bacillus Calmette-Guérin expressing Ag85B-IL-7 fusion protein enhances IL-17A-producing innate $\gamma\delta$ T cells. *Vaccine* 34:2490–2495. <https://doi.org/10.1016/j.vaccine.2016.03.096>.
48. Tang C, Yamada H, Shibata K, Yoshida S, Wajjwalku W, Yoshikai Y. 2009. IL-15 protects antigen-specific CD8⁺ T cell contraction after *Mycobacterium bovis* bacillus Calmette-Guérin infection. *J Leukoc Biol* 86:187–194. <https://doi.org/10.1189/jlb.0608363>.
49. Dejima T, Shibata K, Yamada H, Hara H, Iwakura Y, Naito S, Yoshikai Y. 2011. Protective role of naturally occurring interleukin-17A-producing $\gamma\delta$ T cells in the lung at the early stage of systemic candidiasis in mice. *Infect Immun* 79:4503–4510. <https://doi.org/10.1128/IAI.05799-11>.
50. Murakami T, Hatano S, Yamada H, Iwakura Y, Yoshikai Y. 2016. Two types of interleukin 17A-producing $\gamma\delta$ T cells in protection against pulmonary infection with *Klebsiella pneumoniae*. *J Infect Dis* 214:1752–1761. <https://doi.org/10.1093/infdis/jiw443>.